J. Synchrotron Rad. (1998). **5**, 972–974

Site specification on normal and magnetic XANES of ferrimagnetic Fe_3O_4 by means of resonant magnetic Bragg scattering

Kenji Kobayashi,[a]*† Hiroshi Kawata[a] and Koichi Mori[b]

[a]Photon Factory, Institute of Materials Structure Science, 1-1 Oho, Tsukuba 305, Japan, and [b]Ibaraki Prefectural University of Health Science, 4669-2 Ami, Inashiki 300-03, Japan. E-mail: kenji@sci.cl.nec.co.jp

(*Received 4 August 1997; accepted 12 November 1997*)

Resonant magnetic Bragg scattering (RMBS) for several reflections has been measured at the Fe *K*-edge in Fe_3O_4. The normal and magnetic X-ray absorption near-edge structure (XANES) for two types of Fe ion site (tetrahedral and octahedral) were successfully determined from the analysis of DAFS and RMBS spectra on the assumption that there was an electric dipole transition. The obtained normal XANES for the octahedral site is well explained as a mixture of Fe^{2+} and Fe^{3+} ions, and the characteristic feature of the magnetic XANES at the pre-edge peak is mainly contributed from the Fe^{3+} ion at the tetrahedral site.

Keywords: diffraction anamolous fine structure (DAFS); resonant magnetic Bragg scattering (RMBS); Fe_3O_4; site specification.

1. Introduction

In ferrimagnetic Fe_3O_4 there are two different sites for Fe ions, tetrahedral (T_d) and octahedral (O_h). The normal X-ray absorption near-edge structure (XANES) and magnetic XANES (magnetic circular dichroism, MCD) at these two sites are likely to differ from each other, reflecting the difference in the chemical bonds. XANES and MCD are very useful tools for investigating the electronic and magnetic properties in the unoccupied state. Although several authors have reported on normal and magnetic XANES measurements at the *K*-edge in Fe oxide (*e.g.* Dräger *et al.*, 1988; Maruyama *et al.*, 1995), such methods only give information averaged over the two sites. Recently, Kawata *et al.* (1994) have performed site-specific MCD measurements by using a standing-wave method at the Fe *K*-edge in yttrium iron garnet (YIG). They have shown that the pre-edge structure originates from the Fe^{3+} ions at the T_d site. However, this method can only be applied for a perfect crystal.

Such site-specific measurements can also be performed using resonant enhancements of the anomalous scattering factors in the vicinity of the absorption edge: diffraction anomalous fine structure (DAFS) and resonant magnetic Bragg scattering (RMBS). From DAFS, the anomalous scattering factor due to charge scattering can be obtained by measuring the energy dependence of the Bragg reflection (Vacinova *et al.*, 1995). The RMBS gives the magnetic anomalous scattering factors, which correspond to the magnetic Faraday rotation and MCD (Gibbs *et al.*, 1988).

In this paper, we examine the DAFS and RMBS spectra at the Fe *K*-edge in Fe_3O_4. We have determined the site-specific XANES and MCD spectra for the T_d and O_h sites by fitting experimental DAFS and RMBS data to formalisms based on the $1s$–$4p$ dipole transition. We then compare the results obtained with the average XANES and MCD spectra in Fe_3O_4 and the site-specific MCD in YIG.

2. Experimental

The sample used was a single-crystal in the form of an 8 mm-diameter and 1 mm-thick (110) plate. The experiments were carried out at the beamline 15B of the Photon Factory at the Institute of Materials Structure Science. The white X-rays were monochromated with an Si (331) channel-cut-type monochromator. The sample was put at the centre of the pole pieces of an electromagnet. A magnetic field of 0.37 T was applied perpendicular to the horizontal scattering plane. The Bragg scattering and fluorescence X-ray intensity from the sample were detected by a solid-state detector. The incident X-ray intensity was also monitored with an ionization chamber. The RMBS intensity was defined as $\Delta I/(2I) = (I^+ - I^-)/(I^+ + I^-)$, where I^+ and I^- correspond to the Bragg scattering intensities in the up and down magnetic field directions, respectively. The energy dependence of these intensities was measured around the Fe *K*-edge. All measurements were made at room temperature.

We chose the (444), (440), (620) and (662) reflections. The structure factors F due to the charge scattering can be calculated by

$$\begin{aligned} F_{444} &= 2f(T_d) - 4f(O_h) + 7.8794f(O) \\ F_{440} &= 2f(T_d) + 4f(O_h) + 7.9194f(O) \\ F_{620} &= 2f(T_d) - 0.0604f(O) \\ F_{662} &= -i[4f(O_h) - 7.9194f(O)], \end{aligned} \tag{1}$$

where $f(T_d,O_h)$ represents the atomic form factors of Fe ions for the two crystallographic sites and $f(O)$ represents that of the oxygen ion. The signs of the magnetic form factors for the two Fe sites are opposite because the magnetic moments for two Fe sites are antiparallel-coupled. In this calculation, we used the oxygen parameter $u = 0.379$.

3. Results and discussion

3.1. *DAFS data analysis*

The atomic form factor f is written as

$$f = f_0 + f' + if''. \tag{2}$$

Here, the Thomson scattering factor f_0 is an energy-independent term. On the other hand, the anomalous scattering terms f' and f'' show energy-dependence in the vicinity of an absorption edge. Therefore, we can determine f' and f'' for the T_d and O_h sites by combining the DAFS spectra for several reflections. The imaginary part of the anomalous scattering terms is related to the real part by the Kramers–Kronig relation

$$f'(\omega) = \frac{2}{\pi}\int_0^\infty \frac{\omega' f''(\omega')}{\omega^2 - \omega'^2}\,\mathrm{d}\omega'. \tag{3}$$

First, we determined the anomalous scattering factors due to the charge scattering from the DAFS spectra. Under the assumptions of the kinematical diffraction theory and assuming there is no

† Present address: Fundamental Research Laboratories, NEC Corporation, 34 Miyukigaoka, Tsukuba 305, Japan.

anisotropy of the anomalous scattering factors, the DAFS intensity can be written in the following form,

$$I(\omega) = A\cos^2 2\theta |F|^2/\mu, \tag{4}$$

where $\cos 2\theta$ is the polarization factor, μ is the average absorption coefficient and A is a proportional constant. In (4), the structure factor F is given by

$$F(\omega) = \sum_j \alpha_j \left[f_{0j} + \frac{2}{\pi} \int \frac{\omega' f_j''(\omega')}{\omega^2 - \omega'^2} \mathrm{d}\omega' + i f_j''(\omega) \right], \tag{5}$$

where the sum is taken over the different crystallographic sites labelled by j, and α_j represents the contribution of their atomic form factors to the corresponding reflection index. The integration in (5) was made over as wide an energy range as possible, and the theoretical value of f'' (Sasaki, 1984) was used in the energy region far from the edge. The anomalous scattering terms were determined by minimizing the residual $\Delta^2 = |F|^2_{\mathrm{cal}} - |F|^2_{\mathrm{exp}}$. As shown in Fig. 1, the results match the profile of the experimental data as well as the characteristic feature structure, except in the case of the (440) reflection, where the kinematical diffraction theory is inadequate due to extinction effects. It is worth mentioning that the remarkable feature of the DAFS on the (662) reflection can also be explained; the DAFS intensity increases at the absorption edge because the imaginary part of the anomalous scattering terms is dominant. Fig. 2 shows the anomalous scattering terms obtained for the T_d and O_h sites with the absorption spectra. The absorption spectrum (average f'') has a pre-edge peak A at around 7.112 keV and a resonance feature B in the main absorption region. The imaginary part of the anomalous scattering terms for the T_d site yields a clear pre-edge structure, but the pre-edge feature is weak and broad for the O_h site. This indicates that the pre-edge peak mainly originates from the Fe ions at the T_d site. On the other hand, only the O_h site shows a strong resonance feature. As shown in Fig. 2, this structure around the main edge can be reproduced by two Lorentzian curves with a 5 eV energy shift. Therefore, the shoulders at the lower- and higher-energy sides correspond to the contribution from the Fe^{2+} and Fe^{3+} ions, respectively, in the O_h sites. The estimated chemical shift is consistent with the result reported by Sasaki (1995).

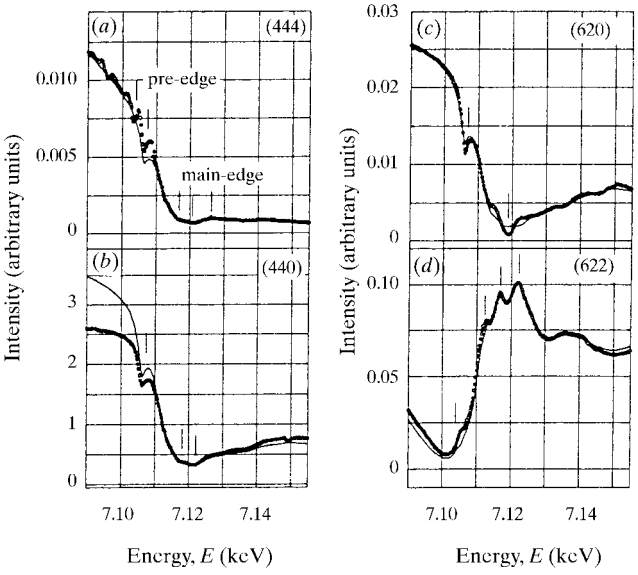

Figure 1
Experimental (circles) and calculated (solid line) DAFS spectra for the (*a*) (444), (*b*) (440), (*c*) (620) and (*d*) (662) reflections at the Fe *K*-edge in Fe_3O_4.

3.2. *RMBS analysis*

Next we determined the magnetic anomalous scattering terms f'^m and f''^m from the RMBS data. On the assumption of a 1*s*–4*p* dipole transition, the scattering amplitude containing the magnetic (spin) scattering is given by (Blume & Gibbs, 1988; Hannon *et al.*, 1988)

$$\begin{aligned}(SA)^2 = &\Big| \sum_j \alpha_j \cos 2\theta (f_{0j} + f_j' + i f_j'') \\ &\mp i \frac{\hbar\omega}{mc^2} \sum_j \alpha_j (\mathbf{k}_f \times \mathbf{k}_i) \mathbf{S}_j(\mathbf{k}) \qquad (6a) \\ &\mp i \sum_j \alpha_j (\mathbf{e}_f^* \times \mathbf{e}_i) \mathbf{z}_j (F_{1,1} - F_{1,-1}) \Big|^2 \\ = &\Big| \sum_j \alpha_j \cos 2\theta (f_{0j} + f_j' + i f_j'') \\ &\mp i \sum_j \alpha_j \sin 2\theta (f_{0j}^m + f_j'^m + i f_j''^m) \Big|^2 \qquad (6b) \\ = &\cos^2 2\theta \left| F_0 + F' + iF'' \right|^2 \\ &\pm 2 \sin 2\theta \cos 2\theta [(F_0 + F') F''^m - F''(F_0^m + F'^m)] \\ &+ \sin^2 2\theta \left| F_0^m + F'^m + iF''^m \right|^2, \qquad (6c)\end{aligned}$$

where $\mathbf{e}_i$ and $\mathbf{e}_f$ are the electric polarization vectors for the incident and scattered X-rays, respectively, $\mathbf{k}_i$ and $\mathbf{k}_f$ are the incident and scattered wavevectors, $\mathbf{z}_j$ is the unit vector in the direction of the magnetization, $(\hbar\omega/mc^2)\mathbf{S}_j(\mathbf{k}) = f_{0j}^m$ is the non-resonant magnetic form factor, $F_{1,1} - F_{1,-1} = f_j'^m + i f_j''^m$ are the magnetic anomalous scattering factors, the double sign ($\mp$) corresponds to up and down magnetic field directions and m denotes the magnetic component. In (6*a*), $F_{L,M}$, where L is the order of the transition and M is the change in angular momentum from the

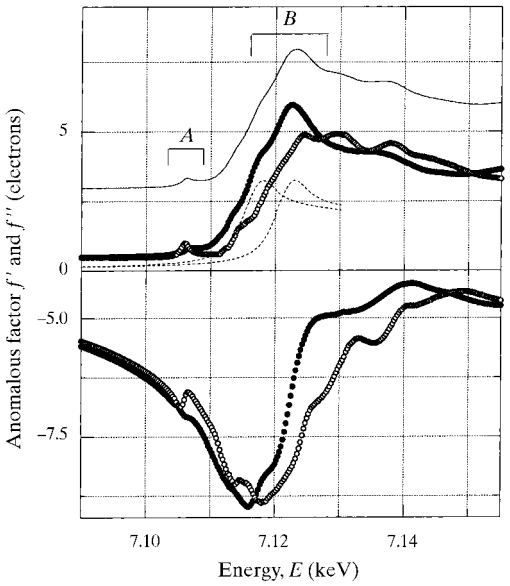

Figure 2
Imaginary (upper panel) and real (lower panel) parts of the anomalous scattering terms obtained for the T_d (open circles) and O_h (closed circles) sites with the average XANES spectra (solid line) at the Fe *K*-edge in Fe_3O_4. The dotted lines represent the Lorentzian curves fitted to the structure for the O_h site in the main-edge region.

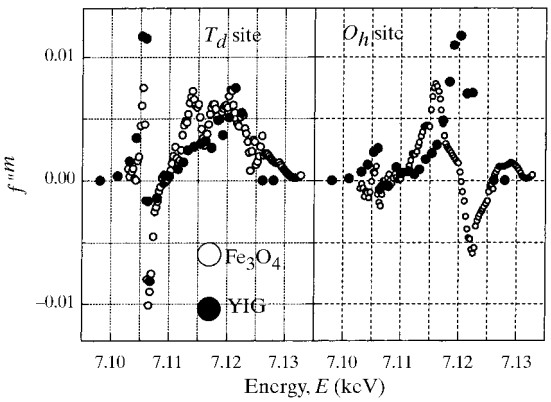

Figure 3
The imaginary part of the magnetic anomalous scattering terms obtained for the T_d (left panel) and O_h (right panel) sites at the Fe K-edge in Fe_3O_4 (open circles) and YIG (closed circles).

initial state to the excited final state, gives the strength of the resonance scattering. Since the third magnetic terms of (6c) can be ignored, the RMBS intensity can be rewritten as

$$\frac{\Delta I}{2I} \simeq 2\tan 2\theta \frac{(F_0 + F')F''^m - F''F'^m - F''F_0^m}{|F|^2_{\text{charge}}}. \qquad (7)$$

We found that the RMBS spectra contained not only the imaginary part of the magnetic anomalous scattering terms corresponding to the MCD but also the real part of the magnetic scattering. In particular, the contribution from the non-resonant magnetic scattering shows an energy-dependence as a result of the coupling with the imaginary part of the anomalous scattering terms due to charge scattering. Since the magnetic anomalous scattering factors are zero well below the absorption threshold, the non-resonant magnetic term can be estimated from (7). We estimate $f_0''^m \simeq 0.19$ for the (662) reflection, in agreement with results of magnetic neutron scattering. Since the structure factors due to the charge scattering were already obtained from the DAFS analysis, we can determine the magnetic anomalous scattering terms from the refinement of the cross terms in (7), expanded using the Kramers–Kronig relationship. To ensure the validity of this analysis, we compared our calculated results with the average MCD in Fe_3O_4 and the site-specific MCD in YIG. Fig. 3 shows the f''^m for the T_d and O_h sites obtained in this analysis compared with the results from the site-specific MCD in YIG. For the T_d site, the profile in Fe_3O_4 shows a behaviour similar to that in YIG; there is a sharp dispersion-type structure at the pre-edge peak, and a weak structure with a positive sign in the wide energy range above the pre-edge peak. A strong magnetic effect at the O_h site appears in the main-edge region for both Fe_3O_4 and YIG. However, the profiles differ from each other. The Fe_3O_4 profile seems to have shifted to the lower-energy side compared with the YIG profile. This shift is probably due to the difference in the electronic configuration at the O_h site between Fe_3O_4 [$(Fe^{3+}Fe^{2+})_{O_h}$] and YIG [$2(Fe^{3+})_{O_h}$]. The estimated energy shift is about 3.7 eV, which is consistent with the chemical shift between $Fe^{2.5+}$ and Fe^{3+}.

4. Conclusions

In this paper, we examined DAFS and RMBS spectra from the Fe K-edge in Fe_3O_4. From our DAFS and RMBS analysis, we determined the anomalous scattering factors for the T_d and O_h sites due to the charge and magnetic scattering. We observed that the pre-edge structure in the XANES spectrum originates from the T_d site, while the resonance feature in the main-edge region originates from the O_h site. In the RMBS analysis, we pointed out the importance of taking into account all of the cross terms between the charge and the magnetic scattering. We also found that the dispersive-type MCD in the pre-edge region is due to Fe ions at the T_d site, while the MCD in the main-edge region is due to the contributions from the O_h and T_d sites. The RMBS spectra at the K-edge could mostly be explained with a formalism based on the assumption of a 1s–4p dipole transition. Therefore, the magnetic resonance scattering amplitude is mainly due to this dipole transition.

We thank Professor S. Todo of the Institute of Solid State Physics for providing us with a good sample of Fe_3O_4, and thank Professor Y. Amemiya at the University of Tokyo and Dr K. Okitsu at the National Research Laboratory of Metrology for the calculation program for the Kramers–Kronig relation. We are also grateful to Professors H. Maruyama and H. Yamazaki at Okayama University for the MCD data. This work was carried out with the approval of the Photon Factory Program Advisory Committee (PAC No. 93G-279).

References

Blume, M. & Gibbs, D. (1988). *Phys. Rev. B*, **37**, 1779–1789.
Dräger, G., Frahm, R., Materlik, G. & Brümmer, O. (1988). *Phys. Status Solidi B*, **146**, 287–294.
Gibbs, D., Harshman, D. R., Isaacs, E. D., McWhan, D. B., Mills, D. & Vettier, C. (1988). *Phys. Rev. Lett.* **61**, 1241–1244.
Hannon, J. P., Trammell, G. T., Blume, M. & Gibbs, D. (1988). *Phys. Rev. Lett.* **61**, 1245–1248.
Kawata, H., Iwazumi, T., Shiotani, N. & Itoh, F. (1994). *Resonant Anomalous Scattering*, edited by G. Materlik, C. J. Sparks & K. Fischer, pp. 557–564. Amsterdam: North Holland.
Maruyama, H., Harada, I., Kobayashi, K. & Yamazaki, H. (1995). *Physica B*, **208–209**, 760–762.
Sasaki, S. (1984). KEK Report, KEK 83–22, KEK, Tsukuba 305, Japan.
Sasaki, S. (1995). *Rev. Sci. Instrum.* **66**, 1573–1576.
Vacinova, J., Hodeau, J. L., Wolfers, P., Lauriat, J. P. & Elkaim, E. (1995). *J. Synchrotron Rad.* **2**, 236–244.